CARBON 90 (2015) 172–180

Available at www.sciencedirect.com

ScienceDirect

journal homepage: www.elsevier.com/locate/carbon

Linear carbon chains encapsulated in multiwall carbon nanotubes: Resonance Raman spectroscopy and transmission electron microscopy studies

N.F. Andrade [a], T.L. Vasconcelos [b], C.P. Gouvea [b], B.S. Archanjo [b], C.A. Achete [b], Y.A. Kim [c], M. Endo [d], C. Fantini [e], M.S. Dresselhaus [f], A.G. Souza Filho [a,*]

[a] Departamento de Física, Universidade Federal do Ceará, P.O. Box 6030, CEP 60455-900, Fortaleza, Ceará, Brazil
[b] Divisão de Metrologia de Materiais, Instituto Nacional de Metrologia, Qualidade e Tecnologia (INMETRO), CEP 25250-020, Duque de Caxias, RJ, Brazil
[c] School of Polymer Science and Engineering, Chonnam National University, 77 Yongbong-ro, buk-gu, Gwangju, 500-757, Republic of Korea
[d] Faculty of Engineering, Shinshu University, 4-17-1 Wakasato, Nagano-shi 380-8553, Japan
[e] Departamento de Física, Universidade Federal de Minas Gerais, Belo Horizonte, MG 30123-970, Brazil
[f] Massachusetts Institute of Technology, Departments of Physics and Electrical Engineering & Computer Science, Cambridge, MA 02139, United States

ARTICLE INFO

Article history:
Received 31 December 2014
Accepted 1 April 2015
Available online 8 April 2015

ABSTRACT

In this paper we report the characterization of linear carbon chains encapsulated in multiwalled carbon nanotubes by using Raman spectroscopy and transmission electron microscopy. The chains are characterized by strong vibrational peaks around 1850 cm^{-1} and both the frequency and intensity of these peaks were found to be dependent on laser excitation energy. Furthermore, resonance Raman spectroscopy was used for constructing the resonance window of the linear carbon chains. The Raman spectroscopy data showed that long chains have lower highest occupied molecular orbital–lowest unoccupied molecular orbital energy gaps and weaker carbon–carbon bonds. Besides the spectroscopy evidence for the linear carbon chain, we used scanning transmission electron microscopy/electron energy loss spectroscopy analysis of the nanotube cross section to unambiguously show the existence of a 1D structure present within the innermost carbon nanotube with an unprecedented clarity compared to previous reports on this kind of system.

1. Introduction

Research on materials made primarily of carbon atoms has received increasing focus and major international investments for several decades, so that these research developments now are at the forefront of the present evolution of science and technology in general. Among the many unique features of this chemical element, a carbon atom is remarkable in its ability to form different types of bonds, which in turn generates materials with a broad and rich variety of physical and chemical properties. The rich chemistry of carbon leads to the possibilities of

* *Corresponding author:* Fax: +55 85 33669450.
E-mail address: agsf@fisica.ufc.br (A.G. Souza Filho).
http://dx.doi.org/10.1016/j.carbon.2015.04.001
0008-6223/

having model systems for all dimensionalities (from 0D to 3D).

In particular, 1D carbon systems consisting of linear carbon chains with *sp* hybridization have attracted the attention of the scientific community for a long time [1,2]. Furthermore, it can be considered that the study of carbon chains is part of the discovery chain going back to fullerenes in the 1980s and carbon nanotubes in the 1990s. It was the study of the formation of long linear carbon chains in interstellar space that contributed to fullerenes coming on the scene [3] and, since then, carbon chains entered several advances involving new carbon nanostructures, such as single- and multiwalled carbon nanotubes [4–8].

Smith et al. [9] found that single wall carbon nanotubes (SWCNTs) can be synthesized to maintain fullerenes encapsulated in the nanotube core, thus leading to so-called "peapods". The ability of carbon nanotubes to encapsulate different entities has been used as a laboratory for obtaining a great variety of nanowires and molecular arrangements, that became possible only because of the strong 1D confinement that a carbon nanotube can provide [10,11]. Thus, the inner space of carbon nanotubes has been recognized as an ideal location to encapsulate and stabilize one-dimensional solids, such as linear carbon chains [12], polyyne $C_{12}H_2$ [13] and $C_{10}H_2$ [14], nanoribbons of WS_2 [15], nanowires [16], and molecules [17], among others.

Long linear carbon chains can be viewed as one-dimensional materials, having a diameter of just one carbon atom. These chains are therefore good candidates for applications in molecular devices regarding both electronic transport [18,19], and as field emitters on the atomic scale [20]. In 2009, stable and rigid carbon atomic chains were experimentally realized by removing carbon atoms, row by row, from graphene through controlled energetic electron irradiation inside a transmission electron microscope [21]. Some methodologies for synthesizing linear carbon chains are described in the literature [22], and one possibility is to grow these chains within the innermost tube of multilayer carbon nanotubes by the arc discharge method, or by using an arc discharge including hydrogen [12], liquid nitrogen [23], and helium [24]. Another possibility to obtain chains is by inserting carbon molecular species within open ended carbon nanotubes followed by a thermal treatment at high temperatures [25,26]. Straight, curved and ring carbon chains have been prepared and observed on graphene by using transmission electron microscopy (TEM) [27]. Recently, Casillas et al. have obtained carbon chains by irradiating few-layer graphene flakes with the electron beam of a TEM at room temperature. By using aberration corrected TEM, they were able to get detailed information about the interaction between the chains as well as the simple and triple bond alternation in the carbon chains [28].

The carbon chains are not stable in air at room temperature and their instability is due to both oxidation and cross-linking phenomena [18]. The encapsulation a of a carbon chain in a nanotube is one way to overcome this instability, and the cavity within the nanotube is therefore ideal for such purposes, insofar as this location offers a possibility for studying these carbon chains directly *in situ*. In the case of multiwall carbon nanotubes (MWCNTs), only the innermost nanotube is effective in protecting and providing the proper space for accommodating the carbon chain [22]. Studies using Raman spectroscopy show that linear carbon chains have intense peaks related to the stretching modes in the 1800–2200 cm^{-1} range. The specific observed frequencies also depend on the chain length and the type of bonding connection, which may be alternating single and triple bonds (polyyne) or only double bonds (polycumulene) [29,30]. Many studies have pointed out the presence of peaks in the lower frequency (1820–1870 cm^{-1}) range when the chains are encapsulated inside carbon nanotubes [12,31]. This down-shift in frequency has been explained as a weakening of the carbon–carbon bond in the chain when the chain is confined inside the core of nanotubes [32]. Furthermore, it has been shown that the observed chain frequency should depend on the number of carbon atoms present in the chain [29]. Therefore, according to some reports in the literature, this peak is interpreted as a spectroscopic characteristic of linear carbon chains encapsulated inside nanotubes.

According to Zhao et al. [33], to form a linear carbon chain inside a carbon nanotube it is necessary for the inner tube to have an internal diameter of 0.7 nm, so that the spacing between the carbon chain and the innermost wall of the tube is the minimal interlayer distance, which is found between two graphene planes separated by the Bernal spacing in graphite. This configuration must allow for carbon chain stabilization, thereby preventing further rearrangement of planes into a different structure. The observation of carbon chains reported in the present work only occurs for a particular set of experimental parameters, thus suggesting that the formation and/or entrapment of linear carbon chains into carbon nanotubes are favored only when certain physical and chemical conditions are used in the sample synthesis, as described here.

The hybrid system Cn@MWCNT, where Cn refers to a carbon chain, gets considerable prominence by being a nanostructure with unique properties and promise for potential applications. It is also hoped that the Cn@MWCNT nanostructure has a Young's modulus and hardness greater than that of carbon fibers and graphite whiskers, so that the mechanical properties of Cn@MWCNT make this system even more attractive to the scientific community [12]. Recently, Liu et al. have investigated the mechanical properties of the carbon chains and they report extreme mechanical performance of these wires with a nominal Young's modulus of 32.71 TPa and a shear modulus of 11.8 TPa [34].

In this paper, we focus on a joint study of both Raman spectroscopy in combination with electron microscopy for a nanosystem consisting of linear carbon chains contained within some of the multiwalled carbon nanotubes. The Cn@MWCNT is discussed here as a model system for a new kind of 1D solid-state nanostructure, due to the presence of long carbon chains within MWCNTs, and for this reason the study of this system gains very special interest. With this work we introduce the first image of the cross section of a system of the Cn@MWCNT type, where we can see the presence of a long wire inside the MWCNT, which we associate with the presence of the carbon chain. So far, the images of such existing systems in the literature were just high resolution transmission electron microscopy (HRTEM) images

[12,18,20,23]. In this paper, we go beyond HRTEM images by showing a scanning transmission electron microscopy (STEM) image of a carbon chain, and we also show results for the characterization of Raman spectra for a carbon chain.

2. Experimental

2.1. Sample preparation

Linear carbon chains encapsulated within the hollow core of multi-walled carbon nanotubes (MWCNTs) were synthesized by the atmospheric arc discharge method, as described in Ref. [6]. A hollow graphite anode (outer diameter = 10 mm, inner diameter = 4 mm) was moved with a speed of 170 mm per minute, while a rod-type carbon cathode (diameter = 35 mm) with a high specific resistivity above 4000 mΩ-cm was rotated with a rate of 155 rpm. The cathode and anode were made of graphite with a purity of 99.99%. Then, by precisely controlling the spacial gap between the electrodes (ca. 1 mm), applying a constant current of 100 A (voltage = 20 V), and using argon gas at a flow rate of 1 L/min along the hollow tube of the graphite cathode, a gray tape spirally arranged on the outer surface of the cathode (width = 3–5 mm, thickness = ca. 175 mm) was obtained. Finally, cooling gas was used to detach the deposited thin tape from the cathode.

2.2. Techniques

We measured the Raman spectra of the samples using a 1.96 eV laser excitation energy. Several Raman spectra were collected at random points over the sample in the nanotube bundle, attempting to check the homogeneity of the sample. We verified that there is no carbon chain at any point along the sample. Raman spectra were acquired in the backscattering geometry with a laser power of about 500 μW. A Witec alpha300R spectrometer was used for measuring the Raman spectra. We used one objective with a 100× amplification and we collected 3 accumulations of 60 s duration for each Raman spectrum at room temperature. For multi-laser resonance Raman measurements, we used a DILOR XY triple-monochromator equipped with a dye laser and an Ar–Kr laser.

HRTEM and scanning transmission electron microscopy (STEM) images were performed using a probe-corrected Titan 80–300 kV (FEI Company) HRTEM instrument working at 80 kV. The low voltage is required in order to avoid damage to the nanotube structure due to the electron beam. The cross-section sample was prepared using a dual beam microscope – Helios Nanolab 650 (FEI Company).

3. Results and discussion

3.1. Raman spectroscopy

The Resonance Raman Spectroscopy (RRS) results show characteristic peaks of the carbon chain Cn at 1850 cm^{-1} for a laser excitation energy E_{laser} of 1.96 eV (Fig. 1). Several measurements were taken at various points along the sample, and in most of the analyzed spectra, a strong intensity

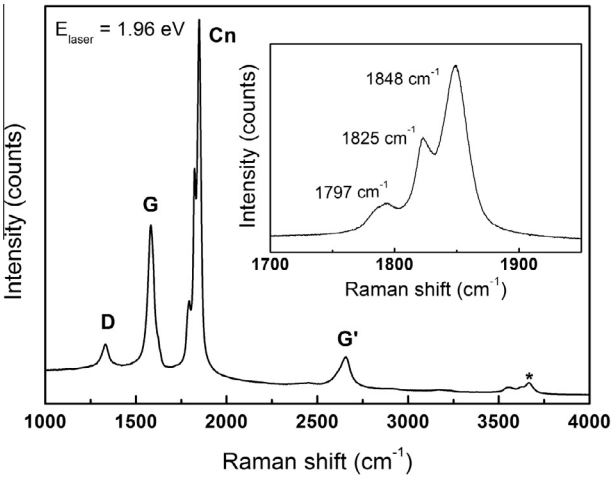

Fig. 1 – Resonance Raman spectrum at room temperature of a Cn@MWCNT bundle excited with E_{laser} = 1.96 eV. The sharp and strong feature at ~1850 cm^{-1} labeled Cn, due to the carbon chain, is shown in greater detail in the inset.

Raman band was found at ~1850 cm^{-1}. Raman peaks characteristic of carbon nanotubes (D, G and G′ bands) were also observed.

A weaker D band intensity was also observed, and this D band peak is indicative of defects present in carbon nanotubes; for example carbonaceous impurities with sp^3 bonds or sp^2 broken bonds on the walls of the nanotubes, indicate that the nanotubes have some degree of disorder. The G band indicates the graphitic nature of the sample, and the G′ band is assigned to a second-order phonon scattering process. The well-defined intensity for both the G band and the G′ band indicates that multiwall carbon nanotubes exhibit a well-ordered stacking of layers. The FWHM with (without) the chain is 43.15 (27.20) cm^{-1} for the G band, and 58.41 (65.86) cm^{-1} for the G′ band. The band centered at 1850 cm^{-1} in Fig. 1 is very intense. It is well known that typical graphitic systems do not exhibit sharp intense Raman peaks in this frequency region. This feature thus cannot be associated with ordinary carbon nanotubes or with any other form of known nanocarbons with sp^2 or sp^3 hybridization. Because of its strong intensity, this 1850 cm^{-1} peak also cannot be attributed to a combination of RBM modes or to tangential modes [35] or to MWCNTs, but must be related to other carbon nanostructures. In this case, we attribute the ~1850 cm^{-1} peak to linear carbon chains present in the innermost core of MWCNTs, as is further discussed below in connection with our HRTEM studies.

The relative intensity between the chain and the G band can be used to qualitatively characterize the concentration of carbon chains present in the sample, since the large intensity of the chain mode indicates that a large amount of chains are expected [22]. According to Fig. 1 the peak intensity associated with the chains is more intense than the G band. The data in Fig. 1 are presented here as an average spectral trace relative to 20 collected spectra. A line profile analysis using Lorentzian fitting functions shows that this feature is formed by a superposition of three peaks around 1797, 1825 and 1848 cm^{-1} of varying intensities and linewidths. These

specific frequencies are not precisely fixed in the sample because there is a wide distribution of intensities and frequency profiles, likely due to a distribution of chains with different lengths as well as different densities of chains contained within a given MWCNT sample. We observed, in the region of 3000–4000 cm^{-1}, the presence of a peak at around 3670 cm^{-1} (marked with * in Fig. 1), and we believe that this "*" mode can be attributed to the second harmonic of the vibration associated with the peak at 1850 cm^{-1}. These results suggest that the narrow band around 1850 cm^{-1} is the result of a vibration from a network of peaks associated with an *sp* carbon chain that is inserted into the core of many MWCNTs in a given bundle sample.

Fig. 2 shows the Raman spectrum, now including some peaks in the low frequency (100–500 cm^{-1}) region (inset). In the 1990s, many Raman experiments were performed on MWCNTs synthesized by the arc discharge method [36] and by chemical vapor deposition (CVD) [37], and in those spectra, no RBM were reported, except in the case of Jantoljak [38]. The MWCNTs obtained in this time period had very large inner diameters d_t when compared to d_t values that are now common for SWCNTs. This might be the reason why it was not possible to observe the RBM modes of MWCNTs in that time period.

The description of RBM modes for MWCNTs, which are similar to RBM modes for SWCNTs, is shown in [33] which confirms that the active Raman modes found in the low frequency region below 400 cm^{-1} originate from the innermost tubes. All these tubes have very small diameters and are the ones which have a considerable Raman intensity due to resonant Raman effects. The frequencies of the RBM vibration ω_{RBM} for multi-walled nanotubes are expected to experience up-shifts of about ~5% compared to the RBM mode associated with SWCNTs [39], due to inter-wall interaction. The smallest diameter carbon nanotube ω_{RBM} observed so far in MWCNTs

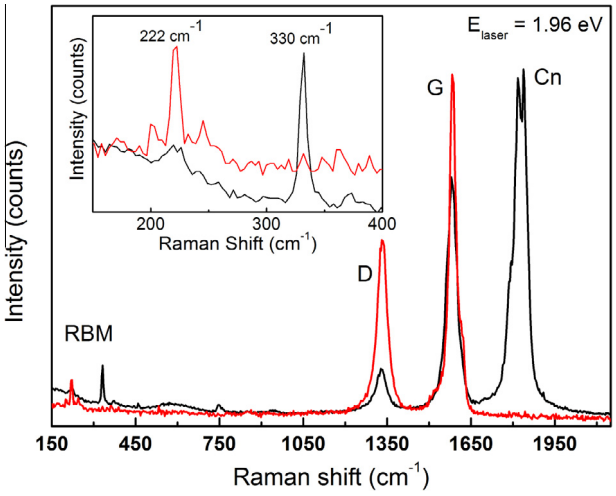

Fig. 2 – Resonance Raman spectra at room temperature for Cn@MWCNTs excited with 1.96 eV laser energy. The spectrum was recorded for a sample region with (black trace) and without (red trace) the carbon chain. The inset shows the RBM region for both spectra. (A colour version of this figure can be viewed online.)

corresponds to a broad feature with a frequency at 570 cm^{-1} and to a tube diameter of 0.4 nm [33].

The presence of a broad peak at around 600 cm^{-1} is seen in the black spectrum and is not seen in the red spectrum of Fig. 2. We relate the $\omega_{RBM} \sim 600\ cm^{-1}$ peak to the 1850 cm^{-1} peak because both these peaks were only observed in the same traces. Similar results that show the simultaneous presence of both the peak at 600 cm^{-1} and 1850 cm^{-1} were also reported in reference [35].

By observing the low frequency region, we have assigned the peaks to the innermost tubes that have very small diameters [33]. The RBM modes are generated when all carbon atoms move in phase in the radial direction, making a breathing vibration of the tube as a whole. In general, the RBM modes are usually strong and are observed in SWCNTs, DWCNTs and TWCNTs [40,41] and in purified MWCNTs [33] with small internal diameters. The presence of many layers damps the vibrations, decreasing their intensities.

Raman studies show that the diameter of an isolated SWCNT is inversely proportional to the RBM frequency [42] by the relation $d_t = 223.75/\omega_{RBM}$, in which d_t is the diameter of a single SWCNT in nanometers, and ω_{RBM} is the RBM frequency in cm^{-1}. When SWCNTs are arranged forming aggregates, their RBM frequencies increase by 5–10% compared with isolated SWCNTs, due to van der Waals interactions between the SWCNTs [43]. In the case of MWCNTs, using resonance Raman scattering and by comparing the RBM of MWCNTs with that of SWCNTs, it was found that the RBM frequencies of MWCNTs "up-shift" in ω_{RBM} by 5% due to interactions between the layers [39]. Using the relationship between the diameter of the isolated SWCNT and the RBM frequency, and by taking into account the "up-shifted" ω_{RBM} by 5%, we can estimate the diameter d_t of the tubes [33] from the RBM spectrum by using $d_t = 223.75/\omega_{RBM} + 0.05\omega_{RBM}$ [33]. So, according to Fig. 2, the frequencies around 222, 330 and 373 cm^{-1} would then be directly related to d_t values of 1.05, 0.71 and 0.63 nm, respectively. We can see in Fig. 2 that the RBM modes of the Raman spectrum for MWCNTs with and without a chain are different from one another. These two kinds of modes are observed at different points along the sample. The black curve (with a chain) shows 3 RBM modes associated with the diameters 1.05, 0.71 and 0.63 nm, and the red curve (without a chain) has just one RBM mode associated with a diameter 1.05 nm. This result indicates that chains are present only when very small diameters of innermost tubes are obtained by the synthesis process with inner tube diameters on the order of 0.7 nm. This very small innermost tube diameter is consistent with the limited space for forming a new tube and for the remaining carbon atoms to arrange themselves to form a chain.

We observed that both the frequency ω_{RBM} and the intensity of this chain were found to be dependent on the laser energy excitation E_{laser}. In an attempt to explore the response of the system over a range of laser excitation energies, we did measurements using different laser lines in order to determine the resonant window of the linear carbon chains. Raman measurements using an Ar–Kr laser with excitation wavelengths at 647, 568, 530, 520, 514, 502, 496, 488 and 476 nm and a dye laser with wavelengths varying continuously in the range 620–560 nm were performed. The results

show a profile associated with the resonant window for the carbon chain peak as shown in Fig. 3(a) and (b). The spectra in this figure were all normalized by the intensity of the G band.

Resonance Raman spectroscopy was used for constructing the resonance window (solid circles) of the linear carbon chains, shown in Fig. 3(b). By fitting the data to a Gaussian curve (solid line in Fig. 3(b)), the maximum intensity obtained is at E_{laser} = 2.13 eV. The dependence between the size or the number of carbon atoms in the carbon chain and the energy of the excitation laser is a qualitatively well-established assumption in the literature [29], being the dependence $E_{laser} \sim 1/L$, where L is the chain length [44]. However, the quantitative value of the energy gap of long one-dimensional carbon chains is not well resolved and it is very sensitive to the calculation method and the value of the energy gap of the chain changes from 0.2 eV to more than 4 eV. To resolve this discrepancy, Al-Backri et al. [45] used the GW many-body approach to calculate the band gap E_{gap} of an infinite carbon chain and they obtained for long chains E_{gap} = 2.16 eV, which is very close to the maximum in the resonance window shown in Fig. 3b. We conclude that a large E_{gap} accesses short chains, where the C–C bond is stronger (higher frequency), while small E_{gap} accesses long chains, where C–C is weaker (lower frequency). The Raman spectroscopy data showed that long chains have lower highest occupied molecular orbital – lowest unoccupied molecular orbital (HOMO–LUMO) energy differences and weaker carbon–carbon bonds. Moreover, it is observed as a shift in the frequency of the carbon chain ω_{Cn} with the laser excitation energy (E_{laser}). We believe that this effect is related to the ability to access different groups of chains at different chain lengths, given the choice in E_{laser}. The frequency (Raman shift) *versus* laser excitation energy obtained in the present study has a behavior shown in Fig. 4. Our resonance Raman scattering results suggest that the chains we measured have the polyyene structure (semiconducting state) and due to the environment into which they are inserted (core of the multilayer nanotube), they are subjected to a certain level of strain due to the van der Waals interaction between the chains and nanotube walls. As discussed above, carbon chains are not observed when the inner core of the nanotube is large. Recently, the strain-induced metal-semiconducting transition in carbon chains has been investigated [19,46]. A temperature-strain phase diagram has been predicted for describing the metal–semiconductor (cumulene–polyyene) transition in a carbon chain [46]. At room temperature, it is expected that a strain of about 3% would stabilize the polyyne structure. This level of strain is compatible with strain due to the van der Waals interaction, which has been responsible for shifting the energies of electronic transitions and vibrational modes of a given carbon nanotube when the nanotubes are in bundles.

Despite the fluctuations existing in Fig. 4, we verify in this figure that for longer wavelengths (lower laser excitation energies), lower ω_{Cn} frequency values are detected in the spectrum for the carbon chains.

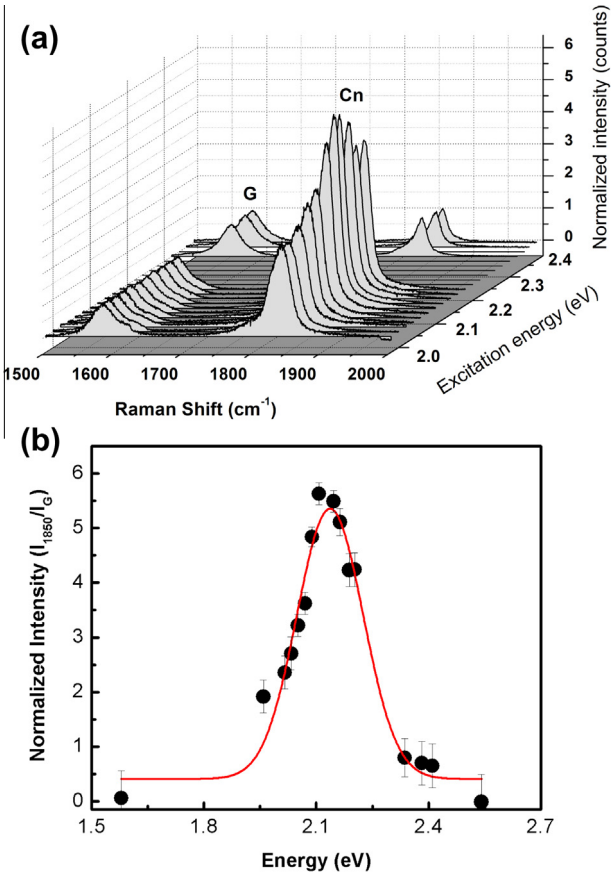

Fig. 3 – (a) Raman spectra of Cn@MWCNTs collected at different laser excitation energies. (b) The resonance window of a carbon chain obtained by the peak intensity of the carbon chain band relative to the G band intensity. The solid red curve is a fit to the data using a Gaussian curve. (A colour version of this figure can be viewed online.)

3.2. *Electron microscopy*

In the previous section we discussed the indirect evidence for the presence of linear carbon chains from Raman spectroscopy. In order to observe such structures in a more direct

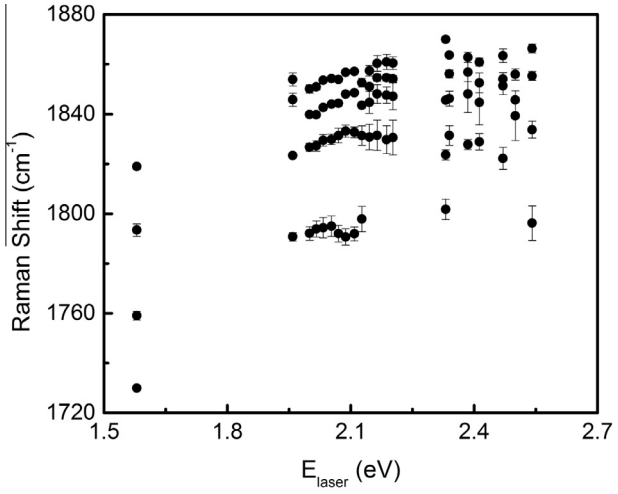

Fig. 4 – Peak frequency of the chain stretching modes vs. the laser excitation energy E_{laser}.

way, we also performed HRTEM studies, aiming to observe and to characterize the carbon chain inside the nanotubes directly. The HRTEM images shown in Fig. 5 suggest the presence of carbon chains inside the MWCNTs.

In Fig. 5a, a TEM (HRTEM) image of one MWCNT, with a 5.3 nm outer diameter, that supports the existence of a C chain at the center of the MWCNT. By inspection of the intensity profile integrated over the dashed box on the TEM image, shown in Fig. 5b, one can count an odd numbers of walls, thus suggesting that there is a 1D object inside the innermost carbon nanotube. It is important to note that the HRTEM images were taken under a defocus condition so that the bright contrast (the bright lines) is assigned to carbon walls. If the opposite were considered (dark lines as carbon walls), one would count an even number of walls and the internal nanotube diameter (about 0.35 nm) would be smaller than the minimal internal diameter predicted by Sawada et al. [47]. Then, considering the bright lines as carbon walls, the diameter of the innermost carbon nanotube is about 0.7 nm, which is a lower diameter value than the upper limit of 1 nm, below which a carbon chain may exist inside a CNT, as reported by Scuderi et al. [16]. The same behavior is observed in the other three HRTEM images (Fig. 5c–e) where the innermost diameters measure between 0.7 and 0.8 nm. Nevertheless, an HRTEM image with this magnification and specimen thickness is basically a phase-contrast image. Therefore, the acquired image is not a direct representation of the sample structure in real space, although in this case the image strongly suggests the existence of a C chain inside the carbon nanotube.

In order to get a more direct confirmation of the presence of a carbon chain inside the carbon nanotube, we prepared a sample using a focused ion beam (see Supplementary Fig. S2 for details on sample preparation). Such a sample allowed us to image the carbon nanotube cross-section with STEM, which generates images that are a sum of *Z contrast* and *diffraction contrast* when performed with a high camera-length and a high-angle annular dark field (HAADF) detector [48,49]. The results are shown in Fig. 6.

In the HAADF mode, the image can be easily interpreted, since interference artifacts are absent, and the fringes seen in Fig. 6a–c are recognized as carbon nanotube walls of a MWCNT. In (a), it is possible to observe the carbon nanotube cross section, whereas in (c) we see its center with a better resolution. In order to make the wall contrast clearer, we have used a digital treatment for generating the image in Fig. 6d (see Supplementary Fig. S1). This digital treatment was performed using an FFT band pass mask between 2 and 4 nm^{-1} on the image shown in Fig. 6c. This FFT mask highlights the carbon nanotube walls since it selects frequencies close to the separation distance between adjacent nanotube walls (about 0.34 nm). This is also seen on the electron diffraction

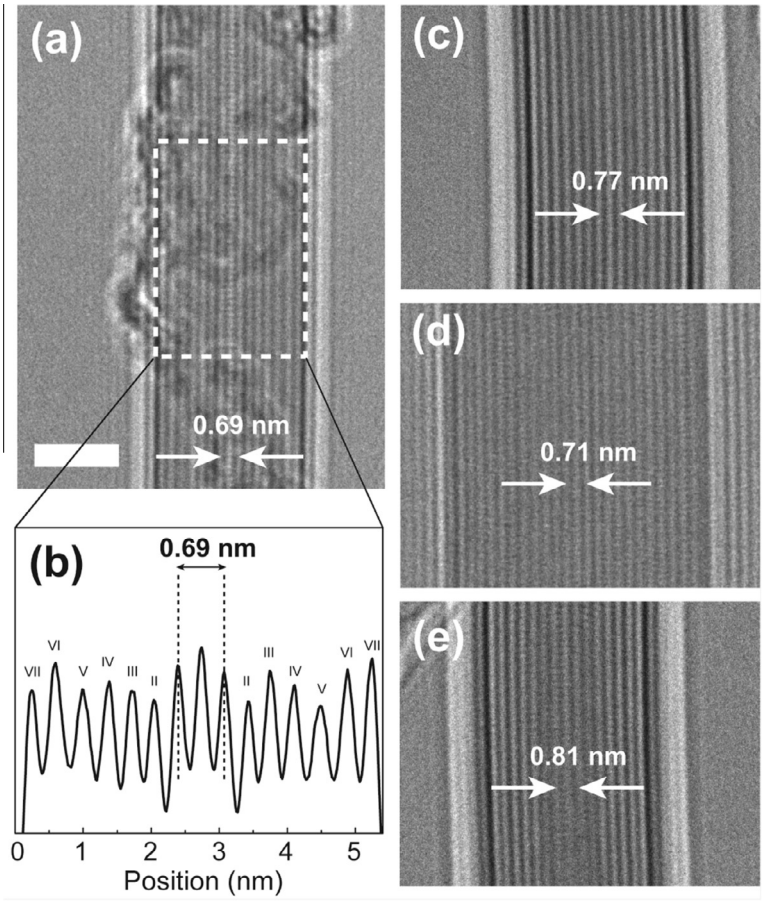

Fig. 5 – (a), (c), (d) and (e) HRTEM images of MWCNTs which contain a central carbon chain. (b) An intensity profile acquired over the carbon nanotube diameter and integrated through the dashed box area shown on image (a). Scale bar: 3 nm.

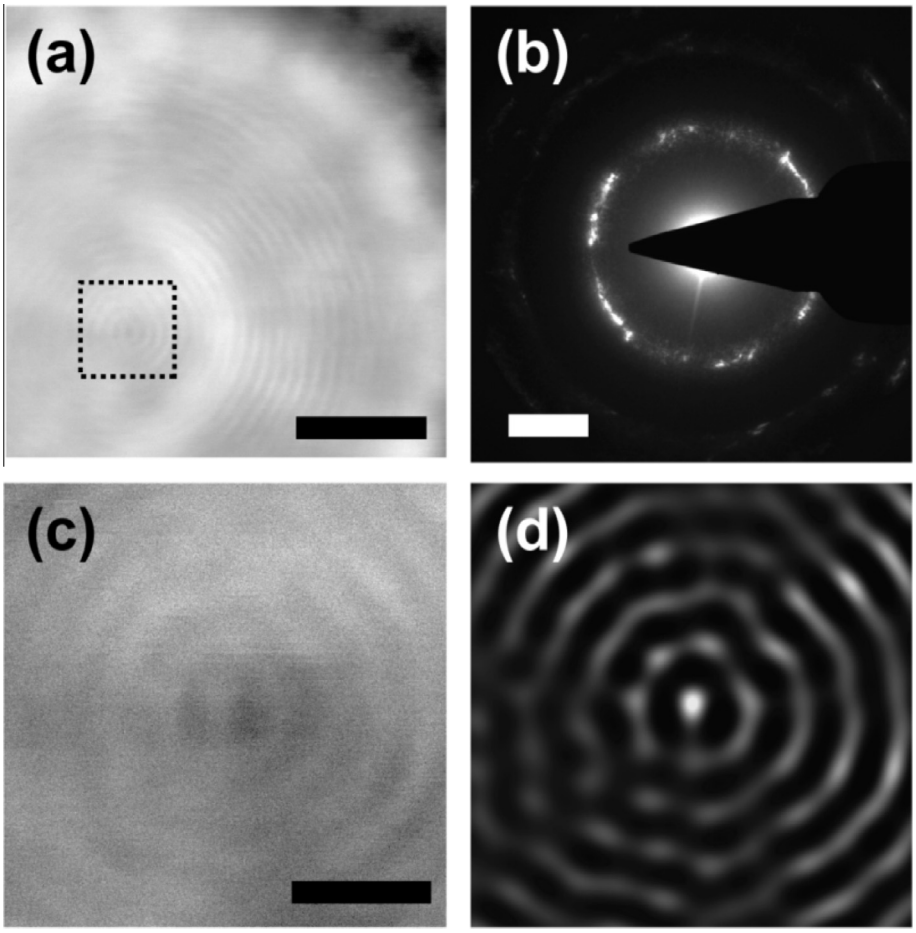

Fig. 6 – (a) High-angle annular dark field (HAADF) image using the scanning transmission electron microscopy (STEM) mode to observe a cross section of a MWCNT containing a carbon chain in the center of the innermost CNT. (b) Selected area electron diffraction of a MWCNT cross section. The area within the dashed square in (a) is zoomed in the HAADF image in the (c) panel. In (d) we see the same image as in (c) but with image treatment. In (d) we have selected frequencies between 2 to 4 nm^{-1} by using a band pass filter in processing the (c) image FFT (fast Fourier transform). The scale bars are 4 nm in (a), 2 nm^{-1} in (b) and 1 nm in (c).

patterning, where an intense signal is measured at 2.9 nm^{-1} (Fig. 6b). By analyzing Fig. 6d it is possible to distinguish the carbon chain inside the innermost carbon nanotube, which has a diameter of 0.82 nm. Nevertheless, the accurate position of the carbon chain inside the CNT may be taken with skepticism since the image of Fig. 6(c) does not show sufficient contrast for accurate analysis, so that image treatment was used to generate Fig. 6(d), but the treated image may preferably enhance the contribution from the central part of the carbon chain imaged in Fig. 6(c), thereby leading to some additional measurement error.

In the same individual MWCNT shown in Fig. 6, we acquired an EELS spectral line along the diameter of this tube in order to analyze the plasmon absorption across the carbon nanotube cross-section. The results are presented in Fig. 7, where in Fig. 7(b) three spectra are shown, two at the carbon nanotube edge (blue and green) and one at the carbon nanotube center, and in Fig. 7(c) a spectrum line summarizing 40 spectra is shown. One can note that, whereas the energy of the π plasmon absorption peak remains at 4.6 eV, the energy of the $\sigma + \pi$ plasmon absorption at the carbon nanotube upper and lower edges shows a red shift of approximately 1 eV when compared to its center. This result corroborates the EELS studies of dispersed MWCNTs in the literature [50–53]. Basically, in the MWCNT center, the bulk plasmon (23–27 eV) is strongly excited, whereas the $\pi \rightarrow \sigma^*$ and $\sigma \rightarrow \pi^*$ surface plasmon (about 14 eV), as well as the $\sigma \rightarrow \sigma^*$ surface plasmon (about 18 eV), are easily excited at the MWCNT edges, causing the apparent energy shift [50–53]. Nevertheless, these results indicate that the carbon chain inside the CNT has no influence on the electron low-loss spectrum.

4. Conclusion

We report a detailed characterization of carbon chains inside CNTs by means of both Raman spectroscopy and electron microscopy techniques. We have used a sample prepared by using focused ion beams and have performed a STEM/EELS analysis of the nanotube cross section. The results shown here unambiguously demonstrate the existence of a 1D structure present within the innermost CNT, with an unprecedented clarity compared to previous reports on this system.

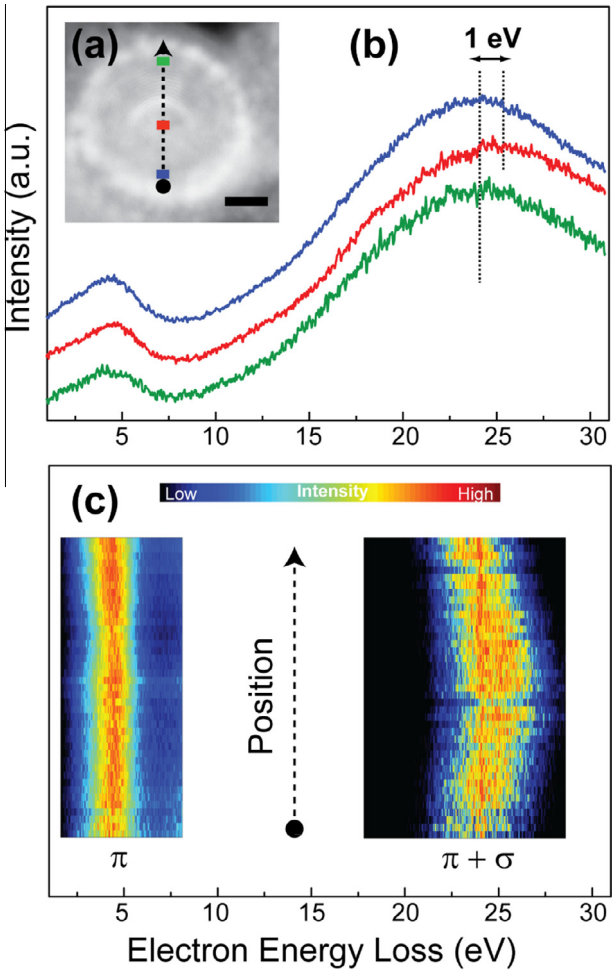

Fig. 7 – Electron energy loss spectrum along the diameter of the nanotube is shown in the inset (a) and is contained in (b). The energy loss for the spectral line is seen in image (a), and three typical spectra are shown in (b), where the blue and green curves show EELS results taken on the MWCNT edges, and the red EELS curve was acquired at the center of the EELS data. In (c), the compilation of all 40 spectra is shown, where colors are related to the normalized intensity. The position of each spectrum can be related to the points on the arrow in (c), which correspond to the arrow in (a), where it can be seen that the maximum of the π plasmon absorption peak remains at 4.6 eV (blue arrow in (c)), whereas the maximum of the $\pi + \sigma$ plasmon absorption peak changes relative to that at the MWCNT center. Scale bar: 5 nm. (A colour version of this figure can be viewed online.)

In addition, the EELS experiment taken along the CNT diameter provides a more complete understanding of the carbon chain influence on the CNT electronic properties.

Acknowledgment

A.G. Souza Filho acknowledges FUNCAP (PRONEX PR2-0054-00022-01-00/11), CNPq-MIT Collaboration agreement and Central Analítica-UFC/CT-INFRA/Pró-Equipamentos CAPES/SisNano-CNPq-MCTI. MSD acknowledges NSF Grant DMR-1004147. YAK acknowledges NRF-2014R1A2A1A10050585.

Appendix A. Supplementary data

Supplementary data associated with this article can be found, in the online version, at http://dx.doi.org/10.1016/j.carbon.2015.04.001.

REFERENCES

[1] Januszewski JA, Tykwinski RR. Synthesis and properties of long [n] cumulenes ($n > 5$). Chem Soc Rev 2014;43:3184–203.
[2] Cataldo F, editor. Polyynes: synthesis, properties, and applications. Boca Raton, FL: Taylor & Francis; 2006.
[3] Kroto HW, Heath JR, ÓBrien, SC, et al. C_{60}: Buckminsterfullerene. Nature (London) 1985;318:162–3.
[4] Iijima S. Helical microtubules of graphitic carbon. Nature 1991;354:56–8.
[5] Iijima S, Ichihashi T. Single-shell carbon nanotubes of 1-nm diameter. Nature (London) 1993;363:603–5.
[6] Kim YA, Muramatsu H, Hayashi T, et al. Catalytic metal-free formation of multi-walled carbon nanotubes in atmospheric arc discharge. Carbon 2012;50:4588–95.
[7] Bethune DS, Kiang CH, De Vries MS. Cobalt-catalysed growth of carbon nanotubes with single-atomic-layer walls. Nature(London) 1993;363:605–7.
[8] Dresselhaus MS, Dresselhaus G, Eklund PC. Science of fullerenes and carbon nanotubes. New York, San Diego: Academic Press; 1996.
[9] Smith BW, Monthioux M, Luzzi DE. Encapsulated C_{60} in carbon nanotubes. Nature (London) 1998;396:323–4.
[10] Chikkannanavar SB, Taubert A, Luzzi DE. Filling single wall carbon nanotubes with metal chloride and metal nanowires and imaging with scanning transmission electron microscopy, vol. 706. MRS Online Proceedings Library; 2001 (pp. Z6.23.1–Z6.23.6).
[11] Hirahara H, Suenaga K, Bandow S, et al. One-dimensional metallofullerene crystal generated inside single-walled carbon nanotubes. Phys Rev Lett 2000;85(25):5384–7.
[12] Zhao X, Ando Y, Liu Y. Carbon nanowire made of a long linear carbon chain inserted inside a multiwalled carbon nanotube. Phys Rev Lett 2003;90(18) (pp. 187401-1–187404-4).
[13] Moura LG, Malard LM, Carneiro MA. Charge transfer and screening effects in polyynes encapsulated inside single-wall carbon nanotubes. Phys Rev B 2009;80(16):161401-1.
[14] Moura LG, Fantini C, Righi A. Dielectric screening in polyynes encapsulated inside double-wall carbon nanotubes. Phys Rev B 2011;83(24) (pp. 245427-1–245427-4).
[15] Wang Z, Zhao K, Li H, et al. Ultra-narrow WS_2 nanoribbons encapsulated in carbon nanotubes. J Mater Chem 2011;21(171):171–80.
[16] Jankovic L, Gournis D, Trikalitis PN. Carbon nanotubes encapsulating superconducting single-crystalline tin nanowires. Nano Lett 2006;6(6):1131–5.
[17] Yanagi K, Moriya R, Cuong NT. Charge manipulation in molecules encapsulated inside single-wall carbon nanotubes. Phys Rev Lett 2013;110(8) (pp. 086801-1–086801-5).
[18] Scuderi V, Scalese S, Bagiante S, et al. Direct observation of the formation of linear C chain/carbon nanotube hybrid systems. Carbon 2009;47(8):2134–7.
[19] Cretu O, Botello-Mendez AR, Janowska I, et al. Electrical transport measured in atomic carbon chains. Nano Lett 2013;13:3487–93.

[20] Wang Z, Ke X, Zhu Z, et al. Carbon-atom chain formation in the core of nanotubes. Phys Rev B 2000;61(4) (pp. R2472–R2474).
[21] Jin C, Lan H, Peng L. Deriving carbon atomic chains from graphene. Phys Rev Lett 2009;102(20) (pp. 205501-1–205501-4).
[22] Sheng L, Jin A, Yu L, et al. A simple and universal method for fabricating linear carbon chains in multiwalled carbon nanotubes. Mater Lett 2012;81:222–4.
[23] Scalese S, Scuderi V, Bagiante S. Controlled synthesis of carbon nanotubes and linear C chains by arc discharge in liquid nitrogen. J Appl Phys 2010;107(1) (pp. 014304-1–014304-6).
[24] Cazzanelli E, Caputi L, Castriota M, et al. Carbon linear chains inside multiwalled nanotubes. Surf Sci 2007;601(18):3926–32.
[25] Malard LM, Nishide D, Dias LG. Resonance Raman study of polyynes encapsulated in single-wall carbon nanotubes. Phys Rev B 2007;76(23) (pp. 233412-1–233412-4).
[26] Shi L, Sheng L, Yu L, et al. Ultra-thin double-walled carbon nanotubes: a novel nanocontainer for preparing atomic wires. Nano Res 2011;4(8):759–66.
[27] Kano E, Takeguchi M, Fujita Jun-ichi, et al. Direct observation of Pt-terminating carbyne on graphene. Carbon 2014;80:382–6.
[28] Casillas G, Mayoral A, Liu M, et al. New insights into the properties and interactions of carbon chains as revealed by HRTEM and DFT analysis. Carbon 2014;66:436–41.
[29] Kastner J, Kuzmany H, Kavan L, et al. Reductive preparation of carbyne with high yield. An *in situ* Raman scattering study. Macromolecules 1995;28(1):344–53.
[30] Kürti J, Magyar C, Balázs A. Vibrational analysis for short carbon chains with alternating and cumulenic structure. Synth Met 1995;71(1–3):1865–6.
[31] Jinno M, Ando Y, Bandow S. Raman scattering study for heat-treated carbon nanotubes: the origin of ≈1855 cm−1 Raman band. Chem Phys Lett 2006;418(1–3):109–14.
[32] Nishide D, Wakabayashi T, Sugai T. Raman spectroscopy of size-selected linear polyyne molecules C2nH2 (*n* = 4-6) encapsulated in single-wall carbon nanotubes. J Phys Chem C 2007;111(13):5178–83.
[33] Zhao X, Ando Y, Qin LC, et al. Radial breathing modes of multiwalled carbon nanotubes. Chem Phys Lett 2002;361(1–2):169–74.
[34] Liu M, Artyukhov VI, Lee H, et al. Carbyne from first principles: chain of C atoms, a nanorod or a nanorope. ACS Nano 2013;7:10075–82.
[35] Jinno M, Bandow S, Ando Y. Multiwalled carbon nanotubes produced by direct current arc discharge in hydrogen gas. Chem Phys Lett 2004;398:256–9.
[36] Ebbesen TW, Ajayan PM. Large-scale synthesis of carbon nanotubes. Nature (London) 1992;358:220–2.
[37] Yacamán MJ, Yoshida MM, Rendón L, et al. Catalytic growth of carbon microtubules with fullerene structure. Appl Phys Lett 1993;62(6):657–9.
[38] Jantoljak H, Salvetat JP, Forró L, et al. Low-energy Raman-active phonons of multiwalled carbon nanotubes. Appl Phys A 1998;67:113–6.
[39] Kataura H, Achiba Y, Zhao X, et al. Resonance Raman scattering of multi-walled carbon nanotubes. Mat Res Soc Symp Proc 2000;593:113–8.
[40] Saito R, Takeya T, Kimura T, et al. Raman intensity of single-wall carbon nanotubes. Phys Rev B 1998;57(7):4145–53.
[41] Alencar RS, Aguiar AL, Paschoal AR, et al. Pressure-induced selectivity for probing inner tubes in double- and triple-walled carbon nanotubes: a resonance Raman study. J Phys Chem C 2014;118(15):8153–8.
[43] Henrard L, Hernández E, Bernier P, et al. Van der Waals interaction in nanotube bundles: Consequences on vibrational modes. Phys Rev B 1999;60(12) (pp. R8521–R8524).
[42] Bandow S, Asaka S, Saito Y, et al. Effect of the growth temperature on the diameter distribution and chirality of single-wall carbon nanotubes. Phys Rev Lett 1998;80(17):3779–82.
[44] Fantini C, Cruz E, Jorio A. Resonance Raman study of linear carbon chains formed by the heat treatment of double-wall carbon nanotubes. Phys Rev B 2006;73(19) (pp. 193408-1–193408-4).
[45] Al-Backri A, Zólyomi V, Lambert CJ. Electronic properties of linear carbon chains: resolving the controversy. J. Chem. Phys. 2014;140(10) (pp. 104306-1–104306-4).
[46] Artyukhov VI, Liu M, Yakobson BI. Mechanically induced metal–insulator transition in carbyne. Nano Lett 2014;14:4224–9.
[47] Sawada S, Hamada N. Energetics of carbon nano-tubes. Solid State Commun 1992;83:917–9.
[48] Pennycook SJ, Nellist PD. Scanning transmission electron microscopy imaging and analysis. Springer; 2011.
[49] Williams DB, Carter CB. Transmission electron microscopy: a textbook for materials science. New York, NY: Springer; 2009.
[50] Stephan O, Kociak M, Henrard L, et al. Electron energy-loss spectroscopy on individual nanotubes. J Electron Spectrosc Relat Phenom 2001;114(116):209–17.
[51] Bursill LA, Stadelmann PA, Peng JL, et al. Surface plasmon observed for carbon nanotubes. Phys Rev B 1994;49(4):2882–7.
[52] Upton MH, Klie RF, Hill JP, et al. Effect of number of walls on plasmon behavior in carbon nanotubes. Carbon 2009;47(1):162–8.
[53] Reed BW, Sarikaya M. Electronic properties of carbon nanotubes by transmission electron energy-loss spectroscopy. Phys Rev B 2001;64(19) (pp. 195404-1–195404-13).